HTD-Vol. 347, National Heat Transfer Conference
Volume 9
ASME 1997

INVESTIGATION OF TRANSPORT PHENOMENA IN MICROCASTING SHAPE DEPOSITION MANUFACTURING VIA OPTIMAL SAMPLING EXPERIMENTS

Kevin Schmaltz, Napoleon Leoni, Prakash Padmanabhan, Cristina Amon, Susan Finger, Lee Weiss

Engineering Design Research Center
Carnegie Mellon University
Pittsburgh, PA

ABSTRACT

A manufacturing technique called microcasting is being developed as part of the Shape Deposition Manufacturing process. Using microcasting, multi-material metal artifacts can be created by successively depositing layers of material into the desired configuration. By combining microcasting with machining operations and the use of sacrificial support materials, complex, multi-material geometries and composite structures can be manufactured. The advantage of the SDM process lies in *directly* generating free-form, near net-shape structures that traditional machining, casting or spraying methods cannot readily achieve.

Ongoing research efforts seek to improve the microcasting process and to minimize manufacturing defects in the deposition layer. Numerical predictions and experimental testing are required to relate microcasting parameters with measurable deposition quality. Previous experiments focused on layers of material; the current work focuses on the individual drops that make up the layers. Adaptive Bayesian surrogate models, in conjunction with optimal sampling, provide an efficient method for selecting and evaluating experiments and exploring the influence of different application parameters.

Sequential updating of surrogates along with optimal sampling for data collection improves surrogate accuracy in our multistage approach and reduces the amount of data collection required. The use of statistical techniques helps the development of an understanding of the relationship between process characteristics and the final quality of the deposition layer.

1. INTRODUCTION

At Carnegie Mellon and Stanford Universities, we are developing a novel manufacturing technique called microcasting as one process for Shape Deposition Manufacturing (SDM). Improving new manufacturing processes such as microcasting requires an understanding of the effects and interactions of process variables on the final quality of the manufactured part. To achieve improved quality of parts, our research combines statistical techniques, numerical simulations of physical models, and experimentation to develop surrogate models for selecting process parameters. This paper reviews the integration of experimental techniques with multistage data collection and optimal sampling. By investigating the effect of process control variables on individual droplet response variables, we seek to gain an understanding of how these individual droplet effects influence the resulting deposited layer.

Microcasting is a hybrid of conventional welding and thermal spray deposition of metals. Thin layers of metal are deposited selectively with the goal of creating parts with better mechanical properties (density, strong interlayer adhesion) than sprayed deposition and without severe distortion of the substrate due to excessive heat (Merz, 1994). In microcasting, drops of molten metal are created in a plasma away from the substrate; the drops fall due to gravity onto the substrate and solidify. A robot moves the microcasting apparatus, or microcaster, to deposit rows of drops to form a layer of metal. Microcasting has been used to deposit several metals including carbon steel, stainless steel, copper, aluminum bronze and invar. A schematic of microcasting is shown in Figure 1.

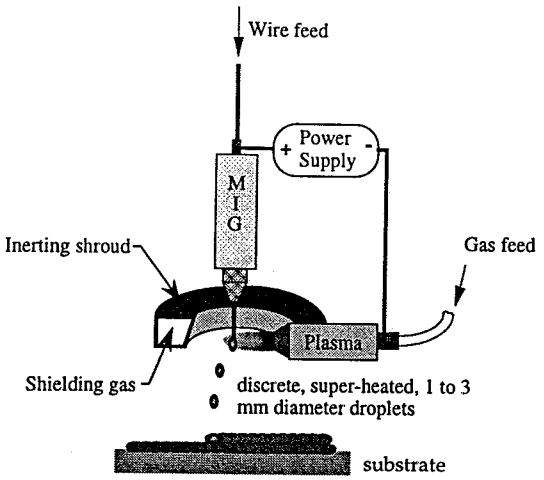

Figure 1: Schematic of the microcasting manufacturing process

Several process parameters are set during microcasting. Typically, only six parameters — plasma current, wire feed rate, standoff, trajectory speed, path spacing, and table angle — are used to control the deposition of a layer. These parameters are shown in Figure 2. Plasma current, standoff, table angle, and wire feed rate are changed to control the individual droplet formation and conditions at impact. The trajectory speed and path spacing are changed to control the formation of an entire layer. Microcasting involves the deposition of molten metal droplets onto substantially cooler substrates, so the key to accurate process modeling and the production of high-quality parts is the ability to predict droplet spreading, solidification, and bonding. Production of high-quality parts also requires the ability to control droplet size, droplet deposition rate, droplet impact velocity, droplet impact temperature, and substrate temperature gradients. These factors combine to influence mechanical strength, material microstructures (and properties), residual thermal stresses, as well as part quality (voids).

The research detailed in this paper focuses on individual droplet experiments that investigate the influence of microcasting process parameters (*e.g.*, plasma current, wire feed rate, torch standoff). These process parameters affect droplet parameters such as size and temperature and hence affect the quality of the resulting deposited layer. The roughness of the substrate also affects the quality of the deposited layer and is included as a parameter in the experiments. These parameters relate the effect on the droplets to the resulting deposited layer. In prior research, we have developed techniques to quantify percentage volume of voids in a deposited layer and have explored the design space of process parameters (Osio, 1996; Padmanabhan, 1996). Because of the large number of parameters involved in the microcasting process, we require an efficient method for selecting the parameter settings to perform the experiments. We have used a multistage approach to data collection, involving design of experiments and optimal sampling. This approach allows us to build surrogate models that embody all available knowledge about the influence of process control parameters on selected responses.

In addition to the experimental investigation presented in this paper, concurrent efforts are underway to improve the microcasting process through modeling and simulation. Through numerical simulations of the impact and solidification of microcast droplets and of the transient thermal stress behavior, we are beginning to understand the interface heat transfer at droplet impact, the spreading behavior of the solidifying droplet, and the overall cooling of both individual droplets and successive layers (Amon *et al.*, 1996a). Process conditions such as the size, temperature and velocity of the droplet as it strikes the substrate are taken as the initial conditions; the simulation output yields the occurrence and extent of partial substrate remelting, and the cooling history of the deposition material. Thermal and mechanical modeling are strongly inter-related because residual stress models depend on spatial-temporal temperatures obtained from the thermal models, and bond strength of successive layers is inherently linked to temperature-controlled substrate remelting. Thermal and mechanical numerical models must be coupled in order to be useful as predictive and investigative tools. Predictive tools will aid in the selection of process parameters, help achieve the desired substrate remelting, and help control residual thermal stresses of the final artifact.

An overview of mechanical issues associated with microcasting is given in Chin *et al.* (1995, 1996), Beuth and Narayan (1996) and Amon *et al.* (1996b). Mechanical modeling provides insight into residual stress build-up during part manufacture and residual stress-driven debonding between deposited layers. Residual stress build-up, inherent to a process based on successive molten material deposition, remelting and solidification, can lead to reduced strength in parts that must withstand substantial mechanical or thermal applied loads, induce undesirable effects such as part warping, loss of edge tolerance, and residual stress-driven inter-layer debonding. Therefore, the goal of stress modeling of microcasting is to understand residual stress build-up and determine process and part design changes to limit stress magnitudes and their unwanted effects.

Our previous work sought to understand how process control parameters influence the quality of a standard part, as measured by the area of voids at given cross sections. Proceeding with a knowledge of the parameter settings that optimize the void area in a deposition layer, we now present results of the variance of individual droplet characteristics (*e.g.*, droplet diameter, falling speed, droplet spreading) with these process control parameters. Minimizing voids requires that successive droplets flow over and wet previously solidified droplets, filling the space between them completely. By gaining insight into the motion of individual droplets and the effect of process parameters on individual droplets, we aim to develop process models that integrate information from physical experiments and numerical simulations (Yesilyurt *et al.*, 1996). In this paper, we construct surrogate models to evaluate the relative effects of the control parameters on droplet behavior using optimal sampling to minimize the experimental data collection required.

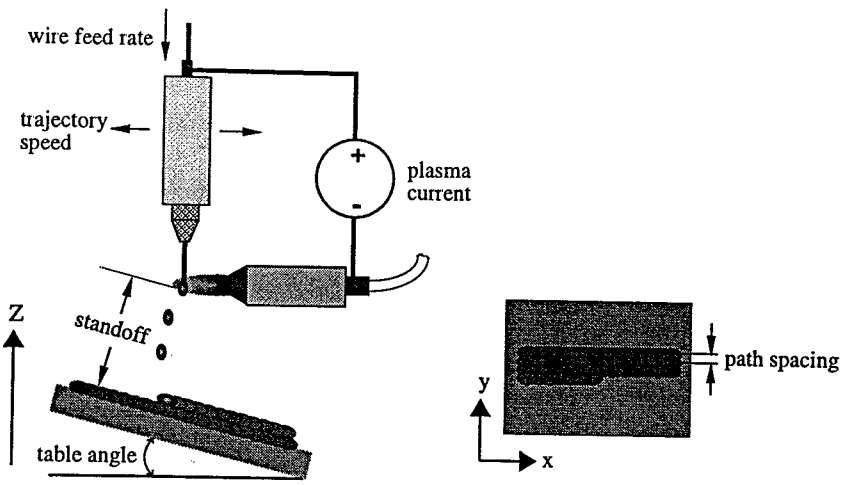

Figure 2: Microcasting parameters

2. Modeling

We use Bayesian surrogates (Currin *et al.*, 1991; Yesilyurt and Patera, 1995) to create models for the microcasting manufacturing process. Surrogate models do not require assumptions about the form of the response but instead are defined in terms of the correlation between sampling sites, allowing for automatic adaptability to the response non-linearities. We build the surrogate models by collecting experimental data in multiple stages (Osio 1996). Initially, we perform screening experiments designed using orthogonal arrays (Owen, 1992). Afterwards, we use optimal sampling to select the sampling points for the next stages of data collection. To visualize surrogate models for high dimensional spaces, we decompose the response in an additive model that includes: the average effect, the first order effects which depend on a single control parameter, the second order cross terms which depend on pairs of design parameters and the high order terms which depend on three or more variables.

In the following example, we illustrate the surrogate methodology by starting with a known analytical function. We show that, by sampling the function using multistage Bayesian analysis, we can create a surrogate for the original function. We will use a function of three variables that all vary between zero and one so our parameter space is the unitary cube [0,1]. To visualize this function as a surface, the value of one of the variables must be fixed, so we have made the function linear in z.

We use an orthogonal array design with 16 sampling points to build our first stage surrogate model. A second stage surrogate is built using optimal sampling over nine new sites. Optimal sampling selects the sites for the next stage that maximize the amount of information that can be gathered from an experiment of the selected size. This is achieved by selecting the new sampling sites based on the degree of non-linearity in each parameter of the surrogate model from the previous stage. At each stage, the surrogate model incorporates all the information gathered in the previous stages, so the second stage surrogate represents the knowledge gathered in a total of 25 sites of the design space. In Figure 3, the analytical function is plotted for a fixed z value ($z=z_o$), and the first and second stage surrogates are shown for the same fixed value, z_o. In Figure 4, we show the main effects of the three variables on the response, calculated from the analytical function, and show the main effects for the first and second stage surrogates. For this example, we can obtain

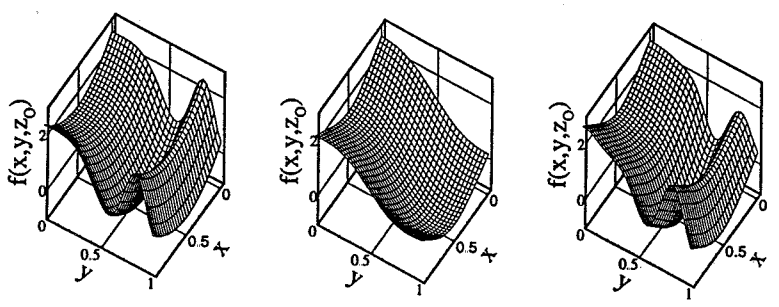

a) analytical function **b) 1st stage surrogate** **c) 2nd stage surrogate**

Figure 3: Carpet plots of the original function with the first and second stage surrogates

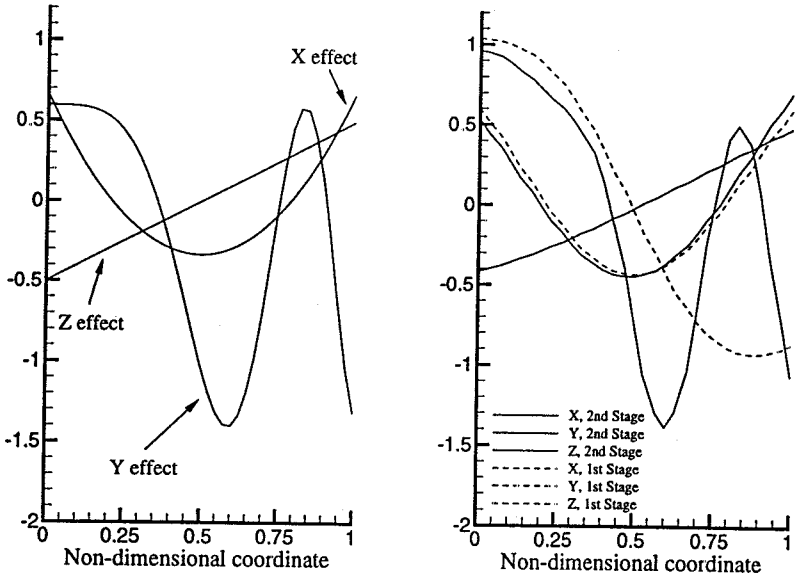

Figure 4: Main effect plot a) analytical b) surrogate

the surrogate model for each stage by adding all the corresponding main effects because there are no interactions among the variables.

This surrogate methodology is used to create a model for the quality of a standard part manufactured using microcasting (Osio and Amon, 1996). The part quality is defined in terms of the voids present in a typical layer deposited by microcasting. Each layer has a height of about 1.25 mm. To assess the quality of the deposited layer, we take values for the layer and average them at three different heights: 0.75 mm, 1.0 mm and 1.25 mm from the top of the substrate. At each height, quality is a function of measured response variables. In this case, quality is defined as the average of four scaled response variables: void count, average void area, standard deviation of void area, and percentage void area. Each response is scaled to lie within a [0,1] range, such that a quality score of 1.0 represents a perfect layer. To measure quality, the layer is photographed and digitally analyzed. The response variables are measured with digital signal processing algorithms.

We conduct the experiments in two stages. The first stage shows the main effects of path spacing and table angle are near linear in this range of parameters. A narrower path spacing improves the quality, as does a higher table angle. The main effects of other parameters exert a nonlinear influence on quality with a maximum value near the center of the range sampled. The magnitude of the main effect of each factor is approximately equal, with no single parameter predominanting. In the second stage of experimentation, the standoff and table angle are maintained at the individual maxima, while other control parameters are varied over a smaller range around the optimal value calculated from the first stage of experimentation. The second stage validates the model created with the results of the first stage and provides a more accurate model of process.

Even though previous experiments provide us with optimal operating points, we still do not understand the interactions among the process parameters that result in better deposition quality. To understand these interactions, we must study individual droplets as well as interactions between droplets. Our current work involves optimal experimentation and analysis to understand the effect of process parameters on individual droplets and the final quality of the parts. The goal of the droplet characterization study is to understand the relationship between the response and control variables summarized in Table 1. Final splat diameter and height are the largest horizontal and vertical dimensions of the solidified, flattened droplet. Transient splat diameter is the largest horizontal dimension experienced by the deforming droplet disk (Figure 6c). Droplet cooling is measured during the solidification of the droplet, along the droplet centerline and near the substrate.

Control Variables	Response Variables
Plasma current	Final splat diameter
Standoff	Final splat height
Wire feed rate	In-flight droplet diameter
Table angle	Maximum transient splat diameter
Substrate material	
Droplet material	Droplet cooling rate

Table 1: Experimental variable summary

3. Experimental Techniques

We have performed experiments to collect data related to the behavior of an individual droplet striking a flat substrate surface and solidifying. The data collected for the droplet include its in-flight size, the transient spreading behavior, the final shape and height, and an estimated cooling rate. The settings for the operating parameters used to generate the droplets for these experiments are determined with the multistage Bayesian surrogate described above. The experimental techniques used to collect individual droplet data include high speed photography to capture in-flight images of the falling droplet and transient spreading, still photography of the resulting solidified droplets, and micrographic characterization to measure the microstructure of the droplets.

For ease in presentation and analysis, we normalize the control variables to the interval [0,1]. Our first stage of data collection consists of a set of screening experiments, using an orthogonal array with three levels and a total of five sampling points for the three dimensional space of each substrate and droplet material combination. To gather data about the process variation, we also repeat three of the experiments at the mid-point settings of the orthogonal array, which corresponds to the mid-values of the control variables in the range being considered. We perform a total of 14 experiments for this initial stage. For each experiment, we deposit one row of four or five droplets for each parameter setting. We build surrogate models for each response variable and perform the functional decomposition to visualize the responses.

Except for the trajectory speed of the robot, all the deposition parameter settings are within the typical operating range used while creating artifacts. Normally, trajectory speeds on the order of 15 to 25 cm per minute are used to generate a continuous line of droplets. Our goal of studying individual droplets requires trajectory speeds in the range of 140 (for stainless steel) to 180 (for copper) cm per minute to ensure that droplets land sufficiently far apart to be considered independent. With these higher trajectory speeds, the droplets are approximately two cm apart and have a flattened diameter of less than 0.75 cm. Measurement of the final droplet shape and spreading are determined by still photography of the deposited droplets. Photographs are taken on a 35 mm black and white 125 plus-X film with indirect diffuse lighting. The photographs are developed and stored on a CD for digital analysis. Digital analysis involves applying a series of filters with PhotoShop™ to obtain a cropped black and white digital image from which the dimensions of the individual droplets are measured.

High speed photography allows us to measure the diameter of the falling droplet before impact and to record the droplet motion upon impact with the flat substrate surface. As with the still photographic experiments, we increase the microcasting deposition path speed above normal path speeds by almost an order of magnitude, leaving a gap of approximately 15 cm between successive droplets. A HYCAM II model 41, high speed 16 mm motion picture camera, capable of film speeds up to 11,000 frames per second records the droplet motion. The camera's drive motor rotates the film take-up spool through a reduction gear, pulling the reel of film across an optical assembly. The film itself acts as a belt, engaging a rotating prism assembly that directs the image onto the passing film. Drag and servo brakes maintain the appropriate tension on the film during recording. To capture the motion of a droplet from impact to solidification, film speeds of up to 5000 frames/second are required. This speed records approximately 25 frames of the droplet between the time of impact with the substrate until the maximum initial droplet spreading is reached, which concludes in 10^{-3} seconds. All ensuing droplet oscillations before final solidification are concluded in approximately 10^{-1} seconds.

High speed filming provides a basis for verification of the numerical model results, as well as critical information on transient droplet/substrate contact angle during spreading, which is a necessary input parameter for the numerical modeling. To see the spreading droplet behavior requires the use of 400 feet of film at 5000 frames per second, providing us with 3.8 seconds of recording time. The camera accelerates the film for the first 50 feet of film length and records the droplets at the set film speed for the remainder of the experiment. Because the droplet's fluid behavior before solidification is also influenced by substrate roughness, our high speed filming experiments include surface roughness as an additional parameter. The substrate surface roughness is either increased or decreased by using coarse (60 grit) or fine (600 grit) sandpaper. The surface roughness is quantified using an arithmetic roughness value (R_a), determined from the surface deviations about the centerline of a filtered profile. The profilometer has a resolution of 0.01 μm.

The final experiment involves a microstructural characterization of the solidified droplet, allowing us to calculate an estimated cooling rate for the droplet material. The spacing between dendrite arms when a liquid alloy solidifies is directly related to the heat flux and the solidification front movement that the particular region of material experiences as it solidifies. By etching the solidified droplet and directly measuring spacing between dendrite arms, we can estimate the cooling rate during solidification at that particular droplet location by comparing the measured spacing values with previously correlated values. Material property consistency and fluid motion depend on cooling rates, and by comparing the resulting microstructure for different application parameters, we seek to gain insight into the effect these parameters have on droplet cooling rates.

4. Results

The combination of control variables investigated in this paper builds on previous work thqt analyzes the quality of parts as a function of control variable combinations from an overall layer viewpoint (Osio and Amon, 1996). We now seek to match individual droplet effects with layer (or part) quality. The analysis of the still photographs of the final shape of the solidified droplets reveals only a slight influence on final droplet shape due to changes of our control variables. For the case of a copper droplet on a steel substrate, the droplet height is most strongly affected by the plasma current;

however, the total variation in the droplet height that the surrogate model predicts due to the plasma current is small compared to the average value of the droplet height (0.0465 cm) estimated from the surrogate for our parameter space. It should also be noted that the estimated standard deviation in the droplet height (0.009 cm) is of the same order as the total variation of the response (0.0013 cm) when the plasma is varied within the range considered, making it difficult to draw definite conclusions about a trend. Process variation has a more important effect on the final height of the droplets than the variation of the parameters themselves. Similar results are found for the droplet splat diameter; the standard deviation in the droplet splat diameter is estimated from our surrogate model to be 0.006 cm around an average main effect or mean value of 0.25 cm. If we compare the standard deviation to the total change in splat diameter due to a variation in plasma current (0.007 cm), we again conclude that process variation has a stronger effect than the control parameters on this response variable.

The set of experiments with the high speed camera uses the same sampling points as the previous experiments, except that we maintain a table angle of zero degrees, due to restrictions with the high speed camera. Table 2 shows the average values of the in-flight microcast droplets (averaged over three to six droplet measurements per experiment). Of the control variables, only plasma current can effect the in-flight droplet diameter. From the film data, we measure the diameter of the droplets and the influence of plasma current on the size of the droplets. These results indicate that the average droplet size decreases for an increasing power level. For the stainless steel, the average droplet is 5.3% smaller at the highest power setting (84A), compared to the lowest setting (56A), while for the copper droplets, the droplet size decreases 10.9% between 39A and 53A.

Figure 5 shows the droplet diameter variation for a copper droplet as a function of plasma current. For this measurement, there

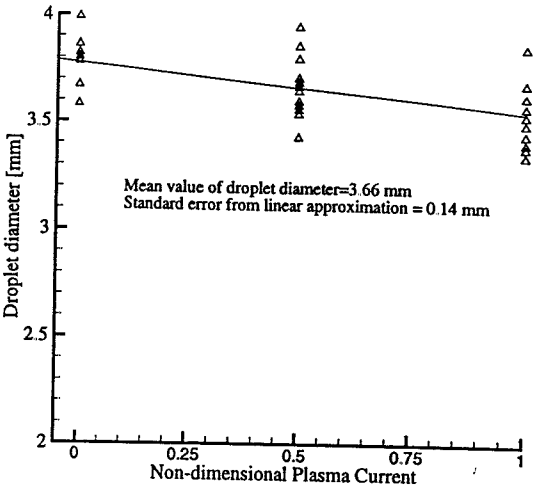

Figure 5: In-flight droplet diameter vs. plasma current for copper droplets

is a clear diminishing trend for the droplet diameter as a function of the plasma current. The total variation of the droplet diameter within the range of study was 0.64 mm around a mean of 3.66 mm. The standard error obtained from fitting a straight line as shown in the figure is on the order of 0.14 mm. The transient droplet spreading response variable is measured using high speed photography. Figure 6 shows four digitized film images, recorded at 5000 frames per second, for a stainless steel droplet striking a stainless steel substrate. The droplet reaches its maximum transient spreading shape in Figure 6c and begins to recoil in Figure 6d. Two types of experiments are performed with the transient spreading response variable.

Droplet Material	Substrate Material	Plasma Current (Amps)	Standoff (inches)	Average Size (mm)
stainless steel	copper	56	4.0	4.49
stainless steel	copper	65	4.0	4.28
stainless steel	stainless steel	65	4.0	4.36
stainless steel	stainless steel	84	4.0	4.25
copper	stainless steel	39	3.0	3.81
copper	stainless steel	53	3.5	3.44
copper	stainless steel	46	4.0	3.58
copper	copper	46	4.0	3.66
copper	copper	53	3.5	3.69
copper	copper	39	3.0	3.83
copper	copper	46	4.0	3.82

Table 2: In-flight droplet diameter

a) on impact b) initial spreading 0016 seconds c) maximum spreading 0.004 seconds d) initial recoiling 0.01 seconds

Figure 6: Stainless steel droplet impinging on a stainless steel substrate (time after impact)

First, we measure the effect of the control variables on transient spreading. Table 3 gives the data from these experiments and Figure 7 shows the surrogate model for this data. Second, with a fixed set of application parameters, we investigate the effect of surface roughness. We performed this second sequence of experiments for varying surface roughness, but used only one plasma power setting and one standoff height (68A and 3.5" for stainless steel droplets, and 42A and 3.5" for copper droplets).

Figure 7 shows the surrogate model for the maximum transient splat diameter. This surrogate model is a function of two parameters: non-dimensional standoff and non-dimensional plasma current. The maximum transient splat diameter is non-dimensionalized by the pre-impact droplet diameter on the plasma current. The surrogate model predicts a response that monotonically increases with the standoff, while no dependence is shown on the plasma current. Therefore, from the fact that the maximum splat diameter changes only with the standoff (*i.e.,* the free fall distance for the droplet), we conclude that dynamic effects are governing the initial maximum spreading.

To determine the influence of surface roughness on transient spreading, stainless steel and copper substrates of varying roughness are prepared. For the copper plate, the smooth region R_a = 0.18 μm, the unmodified region R_a = 0.32 μm, and the roughened region R_a = 1.17 μm. For the stainless steel plate, the smooth region R_a = 0.10 μm, the unmodified region R_a = 0.28 μm, and for the roughened region R_a = 0.81 μm. Droplet spreading is normalized by dividing the maximum spreading diameter by the pre-impact droplet diameter.

Table 4 below shows the results of the measurements. The column labeled *Rough* is the maximum spreading factor for each type of droplet when striking the roughened substrate. The *Normal* and *Smooth* columns represent the unmodified and smoothed substrate surfaces respectively. In all cases, copper droplets undergo a greater degree of spreading than stainless steel droplets, and the smooth substrates permit greater spreading of the droplets than the rougher surface. The reduction in the maximum transient spreading is more pronounced for stainless steel than copper droplets, as shown in the column S/R ratio, which divides the smooth column values by the rough column values. Droplet microstructure is the final data gathered using optimal sampling. The dendrite arm structure of the solid droplets, which is measured for both stainless steel and copper droplets landing on either stainless steel or copper substrates, provides an indication of the cooling rate history. Cooling rate history in turn affects the expected material properties for the resulting layer. For the stainless steel droplets, the structure that best correlates with the cooling rate is the secondary dendrite arm spacing, while for copper, the primary dendrite arm spacing is used. The cooling rate correlation for copper using primary dendrite arm spacing is:

$$\lambda_1 = 306 \cdot R^{-0.36}$$

while the correlation for stainless steel cooling using secondary dendrite arm spacing is:

$$\lambda_2 = 64 \cdot R^{-0.35}$$

where λ is the dendrite arm spacing measured in microns, and R is the effective cooling rate at that location, measured in degrees K per second for the stainless steel (Wolf, 1986) and in degrees K per minute for copper (Bower and Randlett, 1985).

The calculation of cooling rates indicates that on average the copper droplets cool at a higher rate than the stainless steel. When landing on a stainless steel substrate, the average cooling rate for a stainless steel droplet is 5000K/sec., while the copper droplet cooling rate is 5400K/sec. When landing on a copper substrate, the average cooling rate for a stainless steel droplet is 7500K/sec., while the copper droplet cooling rate is 10,500K/sec. The calculated cooling rates are very sensitive to the measured dendrite spacing, and dendrite spacing can vary significantly depending on the location within the droplet where the dendrite is measured. These factors combine to make it difficult to determine qualitative trends from microstructural characterizations to use in a predictive model.

Cooling rates are observed to decrease along the droplet centerline when moving from the substrate interface toward the droplet surface. There is little lateral change in measured cooling rates along the interface from the centerline to the edge of the droplet. Our experiments in which the plasma current setting is varied do not indicate a relationship between the droplet cooling and initial temperature. Due to remelt bonding, heat transfer in microcasting droplets is not limited by interface thermal resistance. Changes to the

Droplet Material	Substrate Material	Plasma Current (Amps)	Maximum Transient Spreading (normalized by in-flight diameter)					
stainless steel	copper	56	1.29	1.28	1.47			
stainless steel	copper	65	1.28	1.38	1.40			
stainless steel	stainless steel	65	1.36	1.31	1.33	1.23		
stainless steel	stainless steel	84	1.23	1.29	1.30	1.30	1.20	1.20
copper	stainless steel	39	1.32	1.25	1.31	1.32	1.29	
copper	stainless steel	53	1.33	1.32	1.31	1.33	1.38	
copper	stainless steel	46	1.44	1.42	1.36	1.39	1.37	1.45
copper	copper	46	1.55	1.55	1.47			
copper	copper	53	1.47	1.45	1.55	1.40	1.51	1.50
copper	copper	39	1.37	1.47	1.45	1.47		
copper	copper	46	1.55	1.55	1.477			

Table 3: Transient spreading under varying control parameters

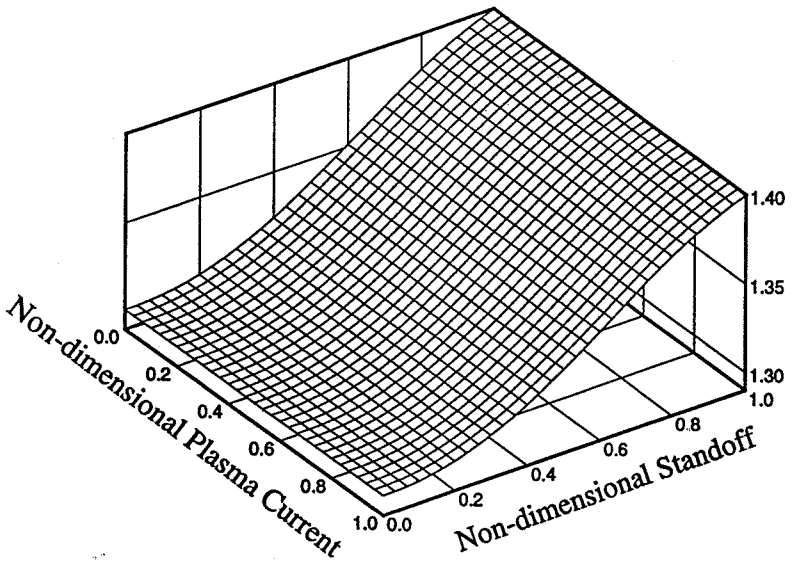

Figure 7: Surrogate model for transient splat diameter vs. normalized plasma current and standoff

Droplet Material	Substrate Material	Maximum Spreading Ratio (Substrate Surface Preparation)			
		Rough	Normal	Smooth	S/R ratio
stainless steel	stainless steel	1.63	1.74	2.00	1.23
stainless steel	copper	1.14	1.44	1.63	1.43
copper	stainless steel	1.56	1.77	1.90	1.21
copper	copper	1.83	1.91	1.95	1.07

Table 4: Transient spreading with varied substrate roughness

plasma power alter the energy transferred to the falling droplet, and larger droplets retain more of this energy. We expected these process parameters to provide an indication of the droplet initial temperature during impact. The superheat present in a droplet influences the cooling conditions (such as the thermal gradient) during solidification, consequently changing the dendrite spacing. We attribute this lack of correlation to the variability of droplet conditions for any given process parameter setting, rather than actual independence between cooling rates and initial temperatures. A more detailed description of the microstructure experiments and analysis is given in Bishop *et al.* (1997).

5. Conclusions

We have created adaptive Bayesian surrogate models of microcasting from data gathered from a variety of experiments (*e.g.*, high-speed and still photography, microstructure analysis), as well as from numerical simulations. By employing a sequential updating of surrogates along with optimal sampling for data collection, we can reduce the data requirements and improve the accuracy of the surrogate using our multistage approach. Bayesian surrogates allow efficient exploration of the influence of different operating parameters (see Table 1) on the quality of microcast artifacts. The use of statistical techniques has allowed us to understand the relationship between the droplet characteristics and the final quality of the deposition layer.

Single droplet experiments provide accurate understanding of molten droplet behavior. While only slight correlations exist between solidified droplet shape (height or diameter) and plasma current, transient droplet spreading is more strongly correlated with both standoff height and substrate surface roughness. High speed photography reveals that droplets strike and return to a near-sessile profile before solidifying. Photography also reveals that a change in plasma current can alter the size of the droplets and that both substrate roughness and standoff height influence the maximum spread of the droplet prior to solidification. The final droplet shape is therefore determined more by droplet properties (surface tension) than by changes in droplet characteristics (size, falling speed) or substrate quality. Drawing conclusions from the resultant microstructure is more difficult. Predicted cooling rates are sensitive to dendrite arm spacing; this spacing varies greatly within a single droplet and across droplets. Copper droplets and copper substrates induce larger cooling rates than stainless steel, due to the comparably greater conductivity of copper.

We have identified operating parameters that minimize the presence of voids. Similarly, we have determined the effect of these parameters on droplet characteristics and behavior. However, from the statistical analysis of our experimental data, clearly the characteristics of single droplets cannot alone explain or predict the occurrence of optimal results. In addition, single droplet characteristics alone do not provide a complete understanding of operating parameter design space. The data gathered from single droplet experiments must be coupled with multi-droplet parameters, such as deposition travel speed and lateral spacing, to create models to correlate deposition parameters with artifact quality (*e.g.*, void area).

Acknowledgments

Financial support by the Advanced Research Project Agency, Grant JFBI92195, the Office of Naval Research, Grant N00014-94-1-0183, the Engineering Design Research Center, a National Science Foundation Center, grant EDC-8943164, and National Science Foundation Grants CTS-9630801 and DMI-9415001 is gratefully acknowledged.

Bibliography

Amon, C.H., Schmaltz, K.S. Merz, R. and Prinz, F.B., 1996a, "Numerical and Experimental Investigation of Interface Bonding Via Substrate Remelting of an Impinging Molten Metal Droplet," *ASME J. of Heat Transfer*, Vol. 118, pp. 164-172,

Amon, C.H., Beuth, J.L., Merz, R., Prinz, F.B. and Weiss, L.E., 1996b, "Shape Deposition Manufacturing with Microcasting: Processing, Thermal and Mechanical Issues," *ASME J. Manufacturing Sciences and Engineering*, under review.

Beuth, J.L. and Narayan, S.H., 1996, "Residual Stress-Driven Delamination in Deposited Multi-Layers," *Int. J. Solids and Structures*, Vol. 33, No. 1, pp. 65-78.

Bishop C.M., Spencer, S.A., Schmaltz, K.S., and Amon, C.H., 1997, "Microstructural Investigation of SDM Microcasting Droplets," *Technical Report EDRC* 24-127-97, Carnegie Mellon University, Pittsburgh, PA.

Bower, T.F. and Randlett, M.R., 1985, "Solidification Structures of Copper Alloy Ingots", *Metals Handbook, Metallography and Microstructures*, K. Mills *et al.*, eds., American Society for Metals, Metals Park, OH, Vol. 9, pp. 637-640.

Chin, R.K., Beuth, J.L. and Amon, C.H., 1995, "Control of Residual Thermal Stresses in Shape Deposition Manufacturing," *Solid Freeform Fabrication Proceedings*, eds. H.L. Marcus *et al.*, pp. 221-228.

Chin, R.K., Beuth, J.L. and Amon, C.H., 1996, "Thermomechanical Modeling of Molten Metal Droplet Solidification Applied to Layered Manufacturing," *Mechanics of Materials*, Vol 24, pp. 257-271.

Currin, C., T. Mitchell, M. Morris and D. Ylvisaker, 1991, "Bayesian Prediction of Deterministic Functions, with applications to the

Design and Analysis of Computer Experiments," *Journal of the American Statistical Association*, Vol. 86, pp 953-963.

Merz, R., 1994, "Shape Deposition Manufacturing," Ph.D. Thesis, Department of Electrical Engineering, Technical University of Vienna, Austria.

Osio, I.G. and Amon, C.H., 1996, "An Engineering Design Methodology with Bayesian Surrogates and Optimal Sampling," *Research in Engineering Design*, Vol. 8, No. 4, pp. 189-206.

Osio, I.G., 1996, "Multistage Bayesian Surrogates and Optimal Sampling for Engineering Design and Process Improvement," Ph.D. Thesis, Department of Mechanical Engineering, Carnegie Mellon University, Pittsburgh, PA.

Owen, A., 1992, "Orthogonal Arrays for Computer Experiments Integration and Visualization," *Statistica Sinica*, Vol. 2, pp 439-452.

Padmanabhan, P., 1996, "Process Planning for Quality: Shape Deposition Manufacturing," Ph.D. Thesis, Department of Mechanical Engineering, Carnegie Mellon University, Pittsburgh, PA.

Wolf, M., 1986, "Strand Surface Quality of Austenitic Stainless Steels: Part 2 Microscopic Solidification Structure" *Ironmaking and Steelmaking*, Vol. 13, No. 5, pp. 258-262.

Yesilyurt, S. and A.T. Patera, 1995, "Surrogates for Numerical Simulations; Optimization of Eddy-Promoter Heat Exchangers," *CMAME*, Vol. 121,pp 231-257.

Yesilyurt, S., C. Ghaddar, M. Cruz and A.T. Patera, 1996, "Bayesian-Validated Surrogates for Noisy Computer Simulations; Application to Random Media," *SIAM Journal of Scientific Computation*.

HTD-Vol. 347

ASME Proceedings of the 32nd

NATIONAL HEAT TRANSFER CONFERENCE

VOLUME 9

• MANUFACTURING AND MATERIALS PROCESSING

presented at

THE 32nd NATIONAL HEAT TRANSFER CONFERENCE
BALTIMORE, MARYLAND
AUGUST 8–12, 1997

sponsored by

THE AMERICAN SOCIETY OF MECHANICAL ENGINEERS, ASME
THE AMERICAN INSTITUTE OF CHEMICAL ENGINEERS, AIChE
THE AMERICAN INSTITUTE OF AERONAUTICS AND ASTRONAUTICS, AIAA
THE AMERICAN NUCLEAR SOCIETY, ANS

edited by

THEODORE L. BERGMAN
UNIVERSITY OF CONNECTICUT

T. H. HWANG
GENERAL ELECTRIC

P. J. PRESCOTT
OWENS CORNING

J. SEYED-YAGOOBI
TEXAS A&M UNIVERSITY

D. A. ZUMBRUNNEN
CLEMSON UNIVERSITY

RANGA PITCHUMANI
UNIVERSITY OF CONNECTICUT

MANOHAR KULKARNI
SOUTHERN ILLINOIS UNIVERSITY

M. K. CHYU
CARNEGIE MELLON UNIVERSITY

S. J. PIEN
ALUMINUM COMPANY OF AMERICA

R. L. MAHAJAN
UNIVERSITY OF COLORADO

THE AMERICAN SOCIETY OF MECHANICAL ENGINEERS
United Engineering Center • 345 East 47th Street • New York, N.Y. 10017